

## Imaging expression of adenoviral *HSV1-tk* suicide gene transfer using the nucleoside analogue FIRU

Dharmin Nanda<sup>1,3</sup>, Marion de Jong<sup>2</sup>, Ronald Vogels<sup>5</sup>, Menzo Havenga<sup>5</sup>, Maarten Driessse<sup>3</sup>, Willem Bakker<sup>2</sup>, Magda Bijster<sup>2</sup>, Cees Avezaat<sup>3</sup>, Peter Cox<sup>2</sup>, Kevin Morin<sup>4</sup>, Ebrahim Naimi<sup>4</sup>, Edward Knaus<sup>4</sup>, Leonard Wiebe<sup>4</sup>, Peter Sillevs Smitt<sup>1</sup>

<sup>1</sup> Department of Neurology, Daniel den Hoed Cancer Centre, University Hospital Rotterdam, PO Box 5201, 3008 AE Rotterdam, The Netherlands

<sup>2</sup> Department of Nuclear Medicine, University Hospital Rotterdam, Rotterdam, The Netherlands

<sup>3</sup> Department of Neurosurgery, University Hospital Rotterdam, Rotterdam, The Netherlands

<sup>4</sup> Faculty of Pharmacy and Pharmaceutical Sciences, University of Alberta, Edmonton, Canada

<sup>5</sup> Crucell Holland BV, Leiden, The Netherlands

Published online: 17 May 2002

© Springer-Verlag 2002

**Abstract.** Substrates for monitoring *HSV1-tk* gene expression include uracil and acycloguanosine derivatives. The most commonly used uracil derivative to monitor *HSV1-tk* gene transfer is 1-(2-fluoro-2-deoxy- $\beta$ -D-arabinofuranosyl)-5-[<sup>125</sup>I]iodouracil (fialuridine; I\*-FIAU), where the asterisk denotes any of the radioactive iodine isotopes that can be used. We have previously studied other nucleosides with imaging properties as good as or better than FIAU, including 1-(2-fluoro-2-deoxy- $\beta$ -D-ribofuranosyl)-5-[<sup>125</sup>I]iodouracil (FIRU). The first aim of this study was to extend the biodistribution data of <sup>125</sup>I-labelled FIRU. Secondly, we assessed the feasibility of detecting differences in *HSV1-tk* gene expression levels following adenoviral gene transfer in vivo with <sup>125</sup>I-FIRU. 9L rat gliosarcoma cells were stably transfected with the *HSV1-tk* gene (9L-tk+). <sup>125</sup>I-FIRU was prepared by radioiodination of 1-(2-fluoro-2-deoxy- $\beta$ -D-ribofuranosyl)-5-tributylstannyl uracil (FTMRSU; precursor compound) and purified using an activated Sep-Pak column. Incubation of 9L-tk+ cells and the parental 9L cells with <sup>125</sup>I-FIRU resulted in a 100-fold higher accumulation of radioactivity in the 9L-tk+ cells after an optimum incubation time of 4 h. NIH-bg-nu-xid mice were then inoculated subcutaneously with *HSV1-tk* (-) 9L cells or *HSV1-tk* (+) 9L-tk+ cells into both flanks. Biodistribution studies and gamma camera imaging were performed at 15 min and 1, 2, 4 and 24 h p.i. At 15 min, the tumour/muscle, tumour/blood and tumour/brain ratios were 5.2, 1.0 and 30.3 respectively. Rapid renal clear-

ance of the tracer from the body resulted in increasing tumour/muscle, tumour/blood and tumour/brain ratios, reaching values of 32.2, 12.5 and 171.6 at 4 h p.i. A maximum specific activity of 22%ID/g tissue was reached in the 9L-tk+ tumours 4 h after <sup>125</sup>I-FIRU injection. Two Ad5-based adenoviral vectors containing the *HSV1-tk* gene were constructed: a replication-incompetent vector with the transgene in the former E1 region, driven by a modified CMV promoter, and a novel replication-competent vector with the *HSV1-tk* gene in E3 driven by the natural E3 promoter. The human glioma cell lines U87MG and T98G were infected with a multiplicity of infection (m.o.i.) of 10. Forty-eight hours later the cells were incubated with <sup>125</sup>I-FIRU and radioactivity was measured in a gamma counter. We found significantly higher levels of radioactivity in both cell lines following infection with the replication-competent vector ( $P < 0.001$ ). NIH-bg-nu-xid mice were then inoculated subcutaneously with U87MG cells. Tumours (approximately 1,000 mm<sup>3</sup>) were injected with 10<sup>8</sup> and 10<sup>9</sup> Infectious Units (I.U.) of either vector. After 48 h, the tracer was injected, followed by gamma camera imaging and direct measurement of radioactivity in the tumours at 4 h p.i. Images and direct measurements indicated increased uptake of tracer with higher I.U. and also demonstrated increased accumulation of tracer in the tumours treated with the replication-competent adenoviral vector ( $P = 0.03$ ). These results demonstrate that <sup>125</sup>I-FIRU in combination with *HSV1-tk* is a valuable tracer for in vivo monitoring of adenoviral gene transfer.

Peter Sillevs Smitt (✉)

Department of Neurology, Daniel den Hoed Cancer Centre, University Hospital Rotterdam, PO Box 5201, 3008 AE Rotterdam, The Netherlands

e-mail: sillevs@neuh.azr.nl

Tel.: +31-10-4391415, Fax: +31-10-4391031

**Keywords:** Gene therapy – Imaging – *HSV1-tk* – Radio-labelled FIRU

**Eur J Nucl Med (2002) 29:939–947**

DOI 10.1007/s00259-002-0839-9

## Introduction

A non-invasive, clinically applicable method for imaging the expression of successful gene transduction in target tissue or specific organs of the body would be of considerable value. It would facilitate the monitoring and evaluation of gene therapy in human subjects by defining the location, magnitude and persistence of gene expression over time [1]. The herpes simplex virus I thymidine kinase reporter gene (*HSV1-tk*) has been explored by several groups for the purposes of imaging reporter gene expression [2, 3, 4, 5, 6, 7, 8, 9].

*HSV1-tk* has a substantially broader specificity than the corresponding mammalian enzyme. For this reason, it has been possible to develop highly effective, low-toxicity anti-herpes virus agents such as acyclovir and ganciclovir. This difference in specificity has made *HSV1-tk* an excellent choice for gene therapy, both as a cytotoxic (e.g. suicide gene therapy) and as a reporter mechanism. The *HSV1-tk*/ganciclovir system is the current standard for suicide gene therapy for cancer [10, 11]. After introduction of the *HSV1-tk* transgene into the cell followed by administration of ganciclovir, the *HSV1-tk* will phosphorylate ganciclovir to ganciclovir monophosphate. Cellular enzymes further metabolise the phosphorylated ganciclovir to ganciclovir triphosphate [12]. Other nucleoside analogues are phosphorylated in a similar manner by *HSV1-tk* [13]. Once phosphorylated, ganciclovir and similar nucleoside analogues are trapped in the cell. The accumulation of the phosphorylated nucleoside analogues in the *HSV1-tk* transfected cells offers the possibility to image the gene transfer by employing radiolabelled pharmaceuticals. A good candidate for imaging *HSV1-tk* with PET is fluorine-18 labelled ganciclovir [8, 9]. However,  $^{18}\text{F}$  has a very short half-life and the production of  $^{18}\text{F}$ -ganciclovir requires proximity to a cyclotron.

The first published compound for *HSV1-tk* imaging in vitro and in animal models was the nucleoside analogue FIAU or fialuridine [1]. Long-term treatment of chronic hepatitis B with pharmacological doses of FIAU proved severely toxic in humans [14]. Incorporation of FIAU in mitochondrial DNA resulted in lactic acidosis, liver failure and pancreatic and neurotoxicity [15]. However, although no toxicity is expected when using tracer amounts of radiolabelled FIAU as calculated by Tjuvavjev et al. [2], systemic toxicity implies phosphorylation by non-transduced tissues and thereby implies some reduction of selectivity for viral TK-expressing tissues. In theory, since FIAU is also phosphorylated by normal tissue, the radiolabelled form can be expected to be phosphorylated and trapped by both normal and transduced tissues. We have studied several related compounds with high specificity for HSV1-TK: FMAU, IV-FRU and FIRU [16, 17]. In vitro toxicity studies revealed that the  $\text{IC}_{50}$  in non-HSV1-TK expressing cell lines was 2–450 times higher for FIRU than for FIAU

while the  $\text{IC}_{50}$  was 2–8 logs higher in HSV1-TK expressing cells, indicating the greater toxicity of phosphorylated FIAU compared with FIRU in replicating cells. We have demonstrated that the uptake ratio of transduced HSV1-TK expressing cells and non-transduced cells is better with FIRU than with FIAU. Using FIRU, we detected no incorporation of the phosphorylated compound into the DNA [16]. This could indicate that the monophosphate is not converted to the di- or triphosphate, or alternatively that the triphosphate is a poor substrate for the DNA polymerase

The nucleoside analogue FIRU therefore does not have potential for suicide gene therapy, but this property makes it an ideal candidate for imaging where information on gene expression is desired without affecting future gene expression. Like other nucleoside analogues, FIRU can be labelled with radioactive iodine isotopes for single-photon emission tomography (SPET) or positron emission tomography (PET) imaging. Iodine-123 was chosen for imaging in these studies because of the 13.3-h half-life and favourable imaging characteristics [18]. In the present study we demonstrate that  $^{123}\text{I}$ -labelled FIRU in combination with a gamma camera is a valuable tracer for imaging *HSV1-tk* gene expression. In addition, with  $^{123}\text{I}$ -FIRU it was possible to demonstrate in vivo the increased *HSV1-tk* expression levels obtained with a replication-competent adenoviral vector as compared with an older E1-deleted adenoviral vector.

## Materials and methods

**Cell culture.** U87MG and T98G human glioma cell lines were purchased from the American Type Culture Collection (ATCC, Manassas, Va.). The rat 9L gliosarcoma brain tumour cell line was a gift from Dr. K.M. Hebeda (Dept. of Experimental Neurosurgery, Free University Hospital Amsterdam, The Netherlands). 9L cells were stably transfected using an *HSV1-tk* carrying retrovirus construct followed by G418 selection [19]. Clones were further selected for GCV sensitivity. All cell lines were grown in Dulbecco's modified Eagle medium (Life Technologies, Breda, The Netherlands) containing 10% foetal bovine serum (Life Technologies), 100 units/ml penicillin and 100  $\mu\text{g}/\text{ml}$  streptomycin (Life Technologies) at 37°C in a 5%  $\text{CO}_2$  atmosphere. The 9L-tk+ cell line was grown in the presence of G418 (250  $\mu\text{g}/\text{ml}$ ) (Life Technologies).

**Vectors.** IG.Ad5.E1+.E3TK is a replication-competent Ad5-based virus in which the *HSV1-tk* gene replaces the gp19K coding sequence in the E3 region (Fig. 1). IG.AdApt.TK is an E1-deleted Ad5-based virus containing the *HSV1-tk* gene driven by the human CMV promoter in the former E1 region. The CMV promoter in IG.AdApt.TK spans nt -735 to nt +95 (numbering according to [20]). Furthermore, IG.AdApt.TK lacks the SV40 intron sequences. The expression cassette is terminated by the SV40 polyadenylation sequence. Figure 1 shows the schematic structure of the two viruses used in this study. Expression levels obtained from the modified CMV promoter are comparable to expression with the natural E3 promoter [21]. Both viruses were produced on PER.C6 cells [22]. After one round of plaque purification, viruses were

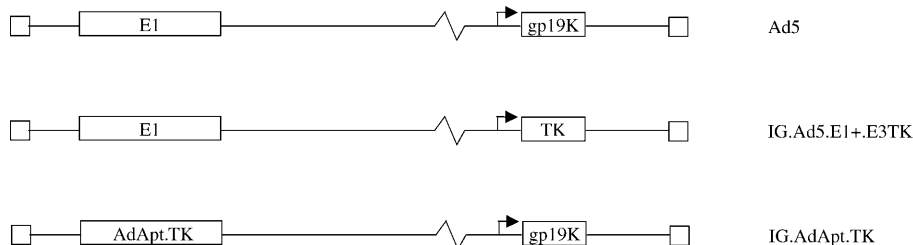


**Fig. 1.** Scheme of replication-competent and non-replicating adenoviral vectors. Ad5 is a wild-type adenovirus 5 vector. IG.Ad5.E1+E3TK is a replication-competent adenoviral vector carrying the *HSV1-tk* gene in E3, replacing the gp19K coding sequence, and is driven by the native E3 promoter. IG.AdApt.TK is an E1-deleted Ad5-based vector containing the *HSV1-tk* gene in the former E1 region driven by an adapted CMV promoter

further amplified on PER.C6 cells. Cells and viruses were harvested 2–3 days following the final amplification in triple layer flasks and viral particles were purified by a two-step CsCl gradient. Virus particles (VP) in purified virus batches were determined by HPLC [23] and Infectious Units (I.U.) were determined by endpoint titration on 911 cells [24]. VP/I.U. ratios were lower than 30 in all cases.

**Synthesis of 1-(2-fluoro-2-deoxy- $\beta$ -D-ribofuranosyl)-5-tributylstannyl uracil (FTBSRU) (precursor compound).** 1-(2-Fluoro-2-deoxy- $\beta$ -D-ribofuranosyl)-5-iodouracil (FIRU) was prepared as previously described [25].  $(\text{Ph}_3\text{P})_4\text{Pd}(0)$  (10 mg, 0.008 mmol) and  $\text{Bu}_3\text{SnSnBu}_3$  (0.16 ml, 0.30 mmol) were added with stirring to a solution of FIRU (4.0 mg, 0.0107 mmol) in dry dioxane (5 ml), and the reaction mixture was stirred for 16 h at 100°C under an atmosphere of argon, at which time TLC analysis indicated the reaction was completed. The catalyst precipitated as a black solid. Removal of the solvent in vacuo and purification of the residue by silica gel column chromatography with methanol-chloroform (1:20, v/v) as eluent afforded FTBSRU as a colourless oil (23 mg, 40% yield).

**Carrier-added radioiodination and purification of FIRU.** Labelling of FIRU was adapted from Wiebe et al. [16]. FTBSRU (100  $\mu\text{g}$ ) was dissolved in 10  $\mu\text{l}$  ethanol/acetic acid (v/v; 50/50), vortexed and microcentrifuged. ICl was dissolved in ethanol/acetic acid (v/v; 50/50) at a concentration of 1 mg/ml, and 25  $\mu\text{l}$  (25  $\mu\text{g}$  ICl) was mixed with 12.5  $\mu\text{l}$  (185 MBq)  $^{125}\text{I}$ . The FTBSRU precursor solution was added, the mixture was incubated at room temperature for 10 min and then the labelling mixture was pushed through an activated Sep-Pak column (activated with 5 ml 2-propanol, rinsed with 5 ml  $\text{H}_2\text{O}$ ). Free iodine is first eluted in 15 ml of  $\text{H}_2\text{O}$ , followed by elution of FIRU in 50% ethanol (v/v ethanol/ $\text{H}_2\text{O}$ ). The FTBSRU precursor eluted in 99% ethanol. The mean labelling yield was 56.4% and the radiochemical purity was >97% (data not shown).

**Cellular uptake of  $^{125}\text{I}$ -FIRU.** 9L and 9L-tk+ cells were plated in six-well plates at a density of  $10^5$  cells per well. When cells had reached 80%–100% confluency, each well was incubated with 2 MBq of  $^{125}\text{I}$ -labelled FIRU for 1, 2, 4, 6, 8 and 24 h. Free radioactive  $^{125}\text{I}$ -FIRU was removed from the cells with two PBS (Life Technologies) washes. In a separate experiment,  $^{125}\text{I}$ -FIRU was washed off the cells 4 h after incubation, followed by collection of

cells, 6, 8 and 24 h after incubation. The cells were then harvested and lysed with 0.1 M NaOH (Life Technologies). Radioactivity in the lysate was determined using a LKB Wallac 1282 Compugamma gamma counter (LKB Instruments, Inc., Gaithersburg, Md.) and corrected for decay. Total protein content was determined in the lysate [26] and radioactivity was expressed as counts per minute/mg protein. All experiments were performed at least in triplicate.

The U87MG and T98G cells were plated in six-well plates at a density of  $10^5$  cells per well. After 24 h the cells were transfected with the replication-competent and replication-incompetent adenoviral vectors carrying the *HSV1-tk* transgene at a multiplicity of infection (m.o.i.) of 10. Forty-eight hours after infection, each well was incubated with 2 MBq of  $^{125}\text{I}$ -labelled FIRU for 4 h. Subsequently, we performed the same procedure as with the 9L and 9L-tk+ cells.

**Animal experiments.** The Institutional Animal Care and Use Committee, in compliance with the Guide for the Care and Use of Laboratory Animals, approved all experimental protocols. Five- to 6-week-old female NIH-bg-nu-xid mice were purchased [27] (Harlan Sprague Dawley Inc., Oxon., UK). Mice were housed three to four per cage and allowed access to food and water ad libitum. After 1 week, 9L, 9L-tk+ or U87MG cells ( $10^7$  cells in 500  $\mu\text{l}$  HBSS; Life Technologies) were inoculated subcutaneously into both flanks. Tumour growth was assessed by measuring bidimensional diameters three times a week with callipers. The tumour volume was determined using the simplified formula of a rotational ellipse ( $\times w^2 \times 0.5$ ) [28].

When the 9L and the 9L-tk+ tumours had reached a volume of approximately 1,000  $\text{mm}^3$ , 3 MBq  $^{125}\text{I}$ -FIRU was injected intravenously into the tail vein. To correlate biodistribution results with gamma camera images, acquisition of images was performed at 15 min and 1, 2, 4 and 24 h after  $^{125}\text{I}$ -FIRU injection. At each time point at least four animals were examined. Mice were anaesthetised with pentobarbital sodium 15 min before acquisition and placed in a spread supine position under the camera. For imaging, a Siemens Rota II gamma camera system (Siemens, Erlangen, Germany) equipped with a low-energy high-resolution collimator was used.

**Biodistribution of  $^{125}\text{I}$ -FIRU.** Biodistribution of  $^{125}\text{I}$ -FIRU was determined 15 min and 1, 2, 4 and 24 h after 3 MBq  $^{125}\text{I}$ -FIRU injections in mice carrying either 9L or 9L-tk+ subcutaneous xenografts. Four mice were examined at each time point. Tumour, brain, thyroid gland, heart, lungs, stomach, kidney, spleen, skin, muscle, femur and blood were collected and weighed, and radioactivity was determined in the gamma counter. The radioactivity is expressed as percentage of the injected dose/g organ (%ID/g) [6].

**Imaging of adenoviral *HSV1-tk* gene transfer into U87MG xenograft.** In vivo evaluation of adenoviral *HSV1-tk* gene transfer was performed in nude mice carrying U87MG xenografts in the right

flank. Once the tumour had reached a volume of 1,000–1,500 mm<sup>3</sup>, animals were injected with replication-competent or -incompetent adenoviral vectors carrying the *HSV1-tk* gene, or with PBS. The adenoviral vectors (10<sup>8</sup> or 10<sup>9</sup> I.U.) were injected into the tumour in 100 µl of PBS. After 48 h, 3 MBq <sup>123</sup>I-FIRU

was injected intravenously and images were acquired 4 h later using the gamma camera with 10 min acquisition time. The animals were sacrificed, the tumour was taken out and weighed, and radioactivity was determined in the gamma counter. Each treatment group consisted of at least four animals.

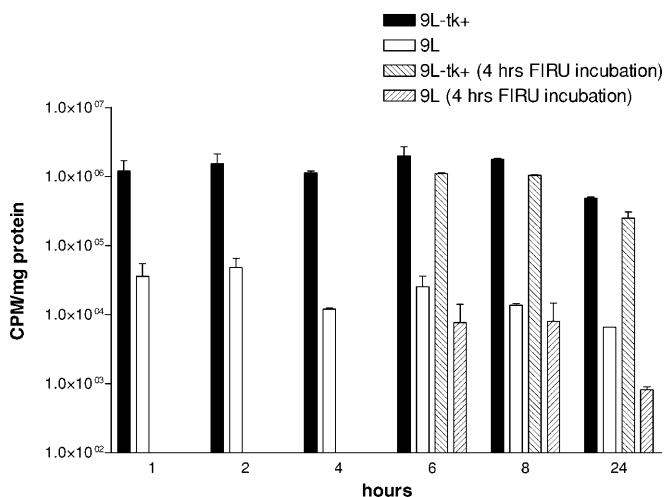
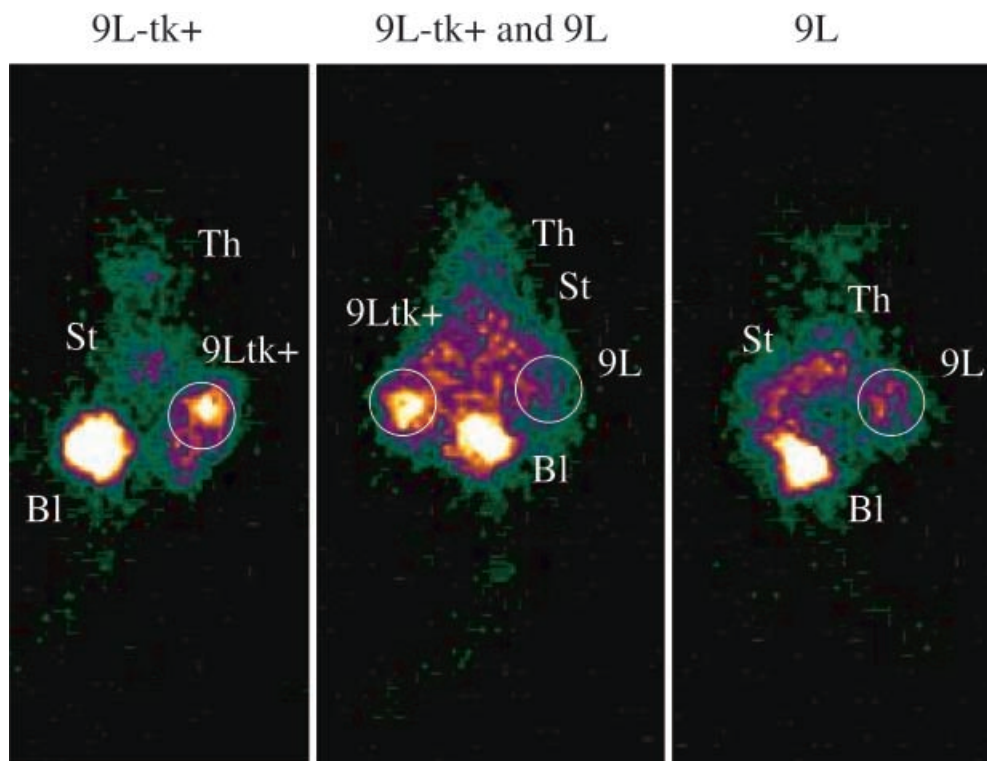


**Fig. 2.** Results of in vitro uptake of <sup>123</sup>I-FIRU in rat 9L glioma cells that constitutively express the *HSV1-tk* gene (9L-tk+) compared with uptake in non-expressing parental cells (9L). Each well was incubated with 2 MBq of <sup>123</sup>I-labelled FIRU for up to 24 h. Cells were harvested and lysed, and the radioactivity was measured in a gamma counter. In a separate experiment, the FIRU was removed from the medium after 4 h of incubation. Uptake of radioactive FIRU was >2 log higher in the 9L-tk+ cells ( $P < 0.001$ ). Removal of <sup>123</sup>I-FIRU from the medium after 4 h of incubation did not affect sequestration of radioactivity in the cells ( $P > 0.05$ ).

**Fig. 3.** Gamma camera images of NIH-bg-nu-xid mice bearing 9L and 9L-tk+ xenografts, 4 h after i.v. administration of 3 MBq <sup>123</sup>I-FIRU. The 9L-tk+ tumours are clearly visualized whereas the 9L control tumours are at background level. Th, Thyroid; St, stomach; Bl, bladder



**Statistical analysis.** Data were analysed using GraphPad Prism version 3.0 software (GraphPad Software, Inc., San Diego, Calif., 1999). The uptake of <sup>123</sup>I-FIRU by the *HSV1-tk* expressing cell line 9L-tk+ and the parental 9L cell line was compared at all time points with and without removal of <sup>123</sup>I-FIRU from the medium, using ANOVA. <sup>123</sup>I-FIRU uptake in U87MG and T98G cells following transfection with replication-competent and non-replicating adenoviral vectors was compared with controls using ANOVA. Post-hoc analysis was performed with Tukey's Multiple Comparison Test. In vivo uptake of <sup>123</sup>I-FIRU by 9L tumours was compared with uptake by 9L tumours at all time points by unpaired Student's *t* test. The medians of in vivo uptake of <sup>123</sup>I-FIRU by U87MG xenografts following infection with replication-competent and non-replicating were compared with each other and with controls using the Kruskal-Wallis test.

## Results

### *Cellular uptake of <sup>123</sup>I-FIRU in constitutively HSV1-tk expressing cells*

Figure 2 demonstrates the selective uptake and retention of <sup>123</sup>I-FIRU by 9L-tk+ cells as compared with the parental 9L cells (ANOVA,  $P < 0.001$ ). The maximum difference between the two cell lines occurs at around 4 h of incubation (>2 log difference). Removal of <sup>123</sup>I-FIRU



**Table 1.** Biodistribution of <sup>123</sup>I-FIRU in NIH-bg-nu-xid mice carrying *HSV1-tk* positive (9L-tk+) or *HSV1-tk* negative (9L) tumours

Time p.i.	9L-tk+ tumour	9L tumour	Specific activity <sup>a</sup>	Liver	Spleen	Kidney	Heart	Femur	Muscle	Thyroid	Stomach	Blood	Brain	Lung	Skin
15 min	13.5±3.2	3.5±0.1	10.0±3.3	2.9±0.3	3.3±0.7	6.4±0.9	3.5±0.3	2.2±0.2	2.6±0.3	4.1±0.7	4.6±0.6	13.7±6.8	0.5±0.2	4.6±0.4	3.7±0.8
1 h	20.1±2.2	2.3±0.2	17.8±2.4	1.4±0.04	1.4±0.1	2.9±0.2	2.5±0.4	1.0±0.1	1.2±0.1	3.1±0.4	5.5±0.7	13.4±3.8	0.6±0.3	2.3±0.2	2.1±0.3
2 h	20.8±2.4	1.4±0.2	19.4±2.6	1.3±0.2	2.1±0.8	2.5±0.6	2.0±0.4	0.9±0.2	1.1±0.4	1.8±0.4	4.6±1.2	2.1±0.5	0.2±0.05	1.7±0.4	2.0±0.8
4 h	23.3±3.4	1.3±0.3	22.0±3.7	1.0±0.3	1.5±0.3	1.5±0.3	1.0±0.2	0.7±0.2	0.7±0.2	2.2±0.3	6.0±1.0	1.2±0.4	0.1±0.04	1.3±0.3	1.2±0.3
24 h	3.1±0.6	0.06±0.01	3.0±0.6	0.04±0.007	0.05±0.004	0.07±0.01	0.05±0.01	0.04±0.005	0.04±0.005	0.3±0.07	0.7±0.14	0.1±0.05	0.03±0.02	0.07±0.005	0.08±0.008

Values are expressed as mean of the %ID/g tissue ±SE (n=4)

<sup>a</sup>“Specific activity” is calculated by subtracting the background activity in *HSV1-tk* negative 9L tumour from the activity in the 9L-tk+ tumour

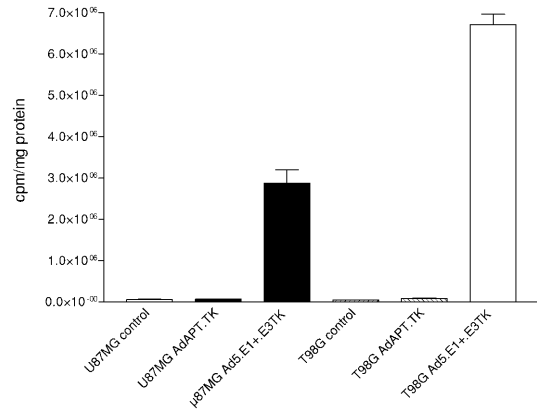


**Fig. 4.** Results of in vitro uptake of <sup>123</sup>I-FIRU in human glioma cells U87MG and T98G. Cells were transfected with replication-competent adenoviral vector IG.Ad5.E1+.E3TK or the non-replicating IG.AdApt.TK at a multiplicity of infection (m.o.i.) of 10. Forty-eight hours after infection, each well was incubated with 2 MBq of <sup>123</sup>I-labelled FIRU for 4 h. Cells were then harvested and lysed, and radioactivity was measured in a gamma counter. Differences in radioactivity between the three treatment groups were highly significant in both cell lines ( $P<0.0001$ ). Uptake of <sup>123</sup>I-FIRU was significantly higher following infection with the replication-competent adenoviral vector as compared with the non-replicating vector ( $P<0.001$ , both cell lines)

**Table 2.** Ratios of <sup>123</sup>I-FIRU uptake in NIH-bg-nu-xid mice carrying *HSV1-tk* positive (9L-tk+) tumours. Tumour/blood, tumour/muscle and tumour/brain ratios were calculated at various time points

	Tumour/muscle	Tumour/blood	Tumour/brain
15 min	5.2	1.0	30.3
1 h	16.3	1.5	32.9
2 h	18.2	10.0	114.3
4 h	32.3	19.4	171.6
24 h	78.7	31.9	122.1

from the medium after 4 h of incubation has no effect on the <sup>123</sup>I-FIRU retention in *HSV1-TK* expressing cells at the later time points (6, 8 and 24 h), indicating entrapment of labelled FIRU in the cells, probably by phosphorylation (Tukey’s Multiple Comparison Test,  $P>0.05$ ).

*In vivo uptake of <sup>123</sup>I-FIRU by constitutively HSV1-tk expressing tumours*

Animals carrying established tumours (either 9L or 9L-tk+) were injected with <sup>123</sup>I-FIRU, and after imaging (Fig. 3) the animals were sacrificed and the radioactivity in the tumours was measured at various time points (Table 1). At all time points, the accumulation of <sup>123</sup>I-FIRU was significantly higher in the *HSV1-tk* expressing 9L-tk+ tumours as compared with the 9L tumours (*t* test:

**Fig. 5.** Gamma camera images of tumour-bearing NIH-bg-nu-xid mice, 4 h after i.v. administration of 3 MBq  $^{123}\text{I}$ -FIRU.

Two days before imaging, the tumours had been injected with PBS (right),  $10^8$  I.U. replication-competent *HSV1-tk* adenovirus (left) or  $10^9$  I.U. of non-replicating *HSV1-tk* adenovirus (middle). The tumour is better visualized in animals treated with the lower dose ( $10^8$  I.U.) of replication-competent *HSV1-tk* adenovirus than in animals injected with a higher dose ( $10^9$  I.U.) of non-replicating virus. Th, Thyroid; Tu, tumour; St, stomach; Bl, bladder

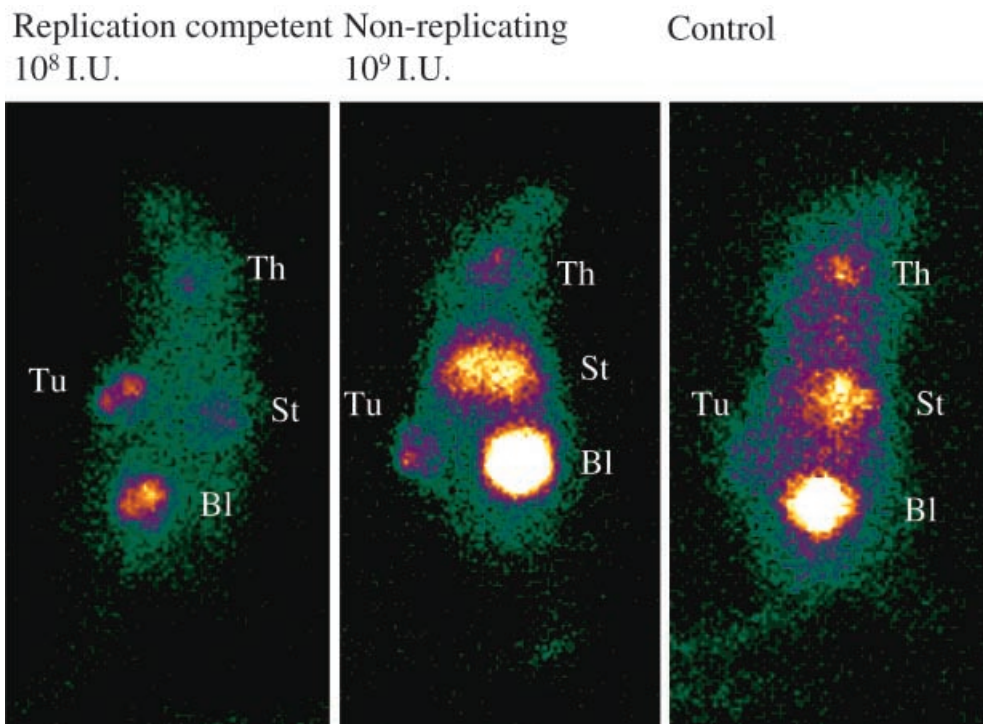


**Table 3.** Tumour uptake of  $^{123}\text{I}$ -FIRU, 2 days after adenoviral injection

	Ad.tk vector				Control	P
	Non-replicating	Replication competent	Non-replicating	Replication competent		
Vector dose	$10^8$ I.U.	$10^8$ I.U.	$10^9$ I.U.	$10^9$ I.U.	–	
Median (range)	1.2 (0.9–2.3)	3.0 (1.9–9.7)	3.0 (1.6–3.8)	4.2 (1.6–8.5)	1.1 (1.1–1.5)	0.03

Values are the ratio of the %ID/g tissue of tumour divided by %ID/g of skin and are expressed as the median (range) of at least four tumours per group. Tumours were injected with a multiplicity

of infection (m.o.i.) of 8 or 9 of either the replication-competent or non-replicating adenoviral vectors containing the *HSV1-tk* gene

15 min,  $P=0.02$ ; 1 h,  $P=0.0002$ ; 2 h,  $P=0.0002$ ; 4 h,  $P=0.0007$ ; 24 h,  $P=0.03$ ). The specific activity in the 9L-tk+ tumours was calculated by subtracting the background activity in *HSV1-tk* negative 9L tumours (Table 1). A maximum specific activity of 22%ID/g tissue was reached 4 h after  $^{123}\text{I}$ -FIRU injection.

#### $^{123}\text{I}$ -FIRU biodistribution

Biodistribution studies again show the high and selective uptake of  $^{123}\text{I}$ -FIRU in *HSV1-tk* expressing 9L tumours as compared with the parental 9L tumours and other tissues (Table 1). In the first hour after injection,  $^{123}\text{I}$ -FIRU levels are highest in peripheral blood and in the kidney (renal excretion). Also, the radioactivity levels in stomach and thyroid are relatively high, indicating in vivo deiodination. The calculated ratios of  $^{123}\text{I}$ -FIRU uptake in

9L-tk+ tumours compared with muscle, blood and brain are depicted in Table 2.

#### Cellular uptake of $^{123}\text{I}$ -FIRU following adenoviral transfection of the *HSV1-tk* gene

Infection of U87MG and T98G cells with replication-competent IG.Ad5.E1+.E3TK at the relatively low m.o.i. of 10 resulted in strong labelling of both cell types with  $^{123}\text{I}$ -FIRU (ANOVA, both cell lines,  $P<0.0001$ ) (Fig. 4). In contrast, labelling was significantly lower with the replication-incompetent vector IG.AdApt.TK when compared directly with the replication-competent vector in both U87MG and T98G cells (Tukey's Multiple Comparison Test,  $P<0.001$  for both cell lines).

*In vivo uptake of <sup>123</sup>I-FIRU following adenoviral intratumoural HSV1-tk gene transfer in U87MG xenografts*

Two days after the injection of both adenoviral vectors into large U87MG s.c. xenograft tumours, we could identify the tumours with a gamma camera (Fig. 5). Following imaging, the animals were sacrificed and the radioactivity in the tumours was determined and expressed as %ID/g tumour tissue. The results of the directly measured radioactivity accumulation in the tumours correlated with the gamma camera images (Fig. 5, Table 3). We then analysed the dose of the adenoviral vectors used on the one hand and the use of replication-competent versus non-replicating virus on the other hand. The differences (Table 3) were significant (Kruskal-Wallis test,  $P=0.03$ ), with higher median <sup>123</sup>I-FIRU uptake in the tumours injected with the replication-competent vector versus the non-replicating vectors, and higher uptake in the tumours injected with the higher dose (m.o.i. 9 vs m.o.i. 8).

## Discussion

Interest in non-invasive imaging for measuring therapeutic transgene expression is growing with the increasing clinical application of gene therapy. Methods used for "molecular imaging" include the use of techniques based on bioluminescence [29] and magnetic resonance imaging and spectroscopy [30], and the use of radionuclides followed by PET or SPET scanning. So far, radionuclide imaging of transgene expression makes use of marker genes encoding cell surface receptors such as the type 2 somatostatin [31] and dopamine type 2 receptors [32], or genes encoding enzymes that selectively metabolise the radionuclide tracer to cause intracellular sequestration [2, 3, 4, 5, 6, 7, 8, 9]. The most frequently used therapeutic gene in cancer gene therapy is the *HSV1-tk* gene [11], and various radiotracers based on uracil nucleosides and acycloguanosine derivatives have been proposed for the non-invasive imaging of *HSV1-tk* gene expression. In a comparative study, we found that FIRU provided optimal performance in terms of selectivity for *HSV1-tk* expressing cells compared with the nucleoside analogues FIAU and IVFRU [16].

In this study we determined the value of <sup>123</sup>I-FIRU for imaging of *HSV1-tk* expression, and found a highly significant accumulation of <sup>123</sup>I-FIRU in constitutively *HSV1-tk* expressing tumours. Following adenoviral transfer of the *HSV1-tk* gene in tumour xenografts, expression of the transgene could be visualised in vivo with a gamma camera. The accumulation of <sup>123</sup>I-FIRU increased with larger amounts of virus injected and the use of a replication-competent adenovirus.

Using the 9L rat glioma cell line stably transfected with the *HSV1-tk* gene, a 100-fold increase in the uptake of <sup>123</sup>I-FIRU compared with the parental cell line was

reached at an optimum of 4 h of incubation. The subsequent removal of <sup>123</sup>I-FIRU from the medium did not result in substantial loss of intracellular <sup>123</sup>I-FIRU, indicating efficient sequestration probably caused by effective phosphorylation.

Biodistribution studies demonstrate selective accumulation of <sup>123</sup>I-FIRU in *HSV1-tk* expressing tumours with 23.3% ID/g of 9L-tk+ tumour tissue, 4 h after tracer injection. This accumulation compares favourably with the 10.5% ID/g of <sup>125</sup>I-FIAU and 0.15% ID/g of <sup>18</sup>F-FHPG [(3-fluoro-1-hydroxy-2-propoxy) methyl guanine] reported for a similar model using the TK expressing murine fibrosarcoma cell line CMS-STK in BALB/c mice [33]. The specific accumulation of radioactivity at 4 h is 22% ID/g (calculated by subtracting the non-specific accumulation of radioactivity in non-transduced 9L tumours from the total radioactivity measured in the 9L-TK tumours) and is higher than the specific accumulation obtained with either <sup>125</sup>I-FIAU (9.8% ID/g) or <sup>18</sup>F-FHPG (0.08% ID/g) [33]. Four hours after tracer injection, the ratios of <sup>123</sup>I-FIRU uptake in tumour to blood, muscle and brain were 19.4, 32.3 and 171.6 respectively. Using <sup>125</sup>I-FIAU, Haubner et al. [6] reported tumour to blood and tumour to muscle ratios at 4 h p.i. of 32.0 and 88.3. In a more recent paper by the same group [33] <sup>125</sup>I-FIAU ratios at 4 h p.i., calculated from Table 1, reveal a tumour to blood ratio of 24.4 and a tumour to muscle ratio of 21. These results indicate that a direct comparison of FIAU and FIRU as substrate for gene imaging is warranted.

The high ratio with normal brain may make FIRU and similar compounds suitable for imaging gene transfer in brain tumours. However, Jacobs et al. [34] demonstrated that iodinated FIAU does not penetrate the intact blood-brain barrier in cats. In a patient with recurrent glioblastoma, substantial levels of <sup>124</sup>I-FIAU-derived radioactivity were found in brain, indicating that the blood-brain barrier in these tumours is disrupted [35]. This study demonstrates the feasibility of obtaining relevant levels of radioactivity to image *HSV1-tk* gene expression with SPET or PET following gene therapy of glioblastomas. However, the demonstrated uptake in non-transduced tumour also indicates that increased background activity may be expected.

The high early radioactivity levels in the kidneys demonstrate the rapid clearance of <sup>123</sup>I-FIRU through the kidneys, similar to <sup>124/125</sup>I-FIAU [33, 35]. Early radioactivity levels in thyroid and stomach indicate some systemic de-iodination of <sup>123</sup>I-FIRU. The in vivo stability of FIRU relative to related 5-substituted nucleosides that do not contain the 2'-fluoro group has been demonstrated before [25].

We then studied the sequestration of <sup>123</sup>I-FIRU in the human glioma cell lines U87MG and T98G following infection with two adenoviral vectors carrying the *HSV1-tk* transgene. IG.Ad5.E1+.E3TK is a replication-competent Ad5-based virus that we constructed to amplify the anti-tumour efficacy of adenovirus-based gene therapy [36].



IG.Ad5.E1+.E3TK results in more efficient cell kill than IG.AdApt.TK, an E1-deleted Ad5-based virus containing the *HSV1-tk* gene driven by the human CMV promoter in the former E1 region [36]. Because rodent cells are not permissive for adenoviral replication, the evaluation of the performance of replication-competent adenoviral vectors requires the use of human cell lines and tumour xenograft models. Here, we have demonstrated that the accumulation of  $^{123}\text{I}$ -FIRU in U87MG and T98G cells was significantly higher following infection with the replication-competent adenovirus compared to the non-replicating vector.

To investigate the possibility of detecting differences in *HSV1-tk* gene expression levels in vivo we injected U87MG xenografts with either  $10^8$  or  $10^9$  I.U. of replication-competent IG.Ad5.E1+.E3TK and non-replicating IG.AdApt.TK. Following injection of  $^{123}\text{I}$ -FIRU, we found that the accumulation of radioactivity was higher in the tumours injected with  $10^9$  I.U. of either virus compared to the tumours injected with  $10^8$  I.U. Also, the tumours injected with the replication-competent virus showed higher radioactivity levels than tumours injected with the non-replicating vector. These findings correlate with images obtained with the clinical gamma camera and demonstrate the feasibility of detecting differences in *HSV1-tk* expression levels using  $^{123}\text{I}$ -FIRU in vivo following adenoviral gene therapy.

In conclusion,  $^{123}\text{I}$ -FIRU accumulates highly selectively in tumour expressing the *HSV1-tk* gene either constitutively or following adenoviral gene transfection. In vivo imaging of the level of *HSV1-tk* expression is possible and will be valuable in both animal studies as in ongoing clinical trials. Future studies will compare the imaging characteristics of tracers that accumulate in the cell following *HSV1-tk* transfection with those obtained with tracers directed at transfected cell surface receptors such as the type 2 somatostatin receptor.

## References

1. Tjuvajev JG, Stockhammer G, Desai R, et al. Imaging the expression of transfected genes in vivo. *Cancer Res* 1995; 55:6126–6132.
2. Tjuvajev JG, Finn R, Watanabe K, et al. Noninvasive imaging of herpes virus thymidine kinase gene transfer and expression: a potential method for monitoring clinical gene therapy. *Cancer Res* 1996; 56:4087–4095.
3. Tjuvajev JG, Avril N, Oku T, et al. Imaging herpes virus thymidine kinase gene transfer and expression by positron emission tomography. *Cancer Res* 1998; 58:4333–4341.
4. Tjuvajev JG, Chen SH, Joshi A, et al. Imaging adenoviral-mediated herpes virus thymidine kinase gene transfer and expression in vivo. *Cancer Res* 1999; 59:5186–5193.
5. Tjuvajev JG, Joshi A, Callegari J, et al. A general approach to the non-invasive imaging of transgenes using cis-linked herpes simplex virus thymidine kinase. *Neoplasia* 1999; 1:315–320.
6. Haubner R, Avril N, Hantzopoulos PA, Gansbacher B, Schwaiger M. In vivo imaging of herpes simplex virus type 1 thymidine kinase gene expression: early kinetics of radiolabelled FIAU. *Eur J Nucl Med* 2000; 27:283–291.
7. Gambhir SS, Barrio JR, Wu L, et al. Imaging of adenoviral-directed herpes simplex virus type 1 thymidine kinase reporter gene expression in mice with radiolabeled ganciclovir. *J Nucl Med* 1998; 39:2003–2011.
8. Gambhir SS, Barrio JR, Phelps ME, et al. Imaging adenoviral-directed reporter gene expression in living animals with positron emission tomography. *Proc Natl Acad Sci U S A* 1999; 96:2333–2338.
9. de Vries EF, van Waarde A, Harmsen MC, Mulder NH, Vaalburg W, Hospers GA. [(11)C]FMAU and [(18)F]FHPG as PET tracers for herpes simplex virus thymidine kinase enzyme activity and human cytomegalovirus infections. *Nucl Med Biol* 2000; 27:113–119.
10. Sobol RE, Shawler D, Dorigo O, Gold D, Royston I, Fakhrai H. Immunogene therapy of cancer. In: Sobol RE, Scanlon KJ, eds. *The Internet book of gene therapy*. Stamford, Conn.: Appleton & Lange; 1995:175–180.
11. Nanda D, Driesse MJ, Sillevs Smitt PAE. Clinical trials of adenoviral-mediated suicide gene therapy of malignant gliomas. *Progr Brain Res* 2001; 132:709–720.
12. Moolten FL. Drug sensitivity (“suicide”) genes for selective cancer chemotherapy. *Cancer Gene Therapy* 1994; 1:279–287.
13. Balzarini J, Bohman C, Walker RT, De Clercq E. Comparative cytostatic activity of different antiherpetic drugs against herpes simplex virus thymidine kinase gene-transfected tumor cells. *Mol Pharmacol* 1994; 45:1253–1258.
14. McKenzie R, Fried MW, Sallie R, et al. Hepatic failure and lactic acidosis due to fialuridine (FIAU), an investigational nucleoside analogue for chronic hepatitis B [see comments]. *N Engl J Med* 1995; 333:1099–1105.
15. Cui L, Yoon S, Schinazi RF, Sommadossi JP. Cellular and molecular events leading to mitochondrial toxicity of 1-(2-deoxy-2-fluoro-1-beta-D-arabinofuranosyl)-5-iodouracil in human liver cells. *J Clin Invest* 1995; 95:555–563.
16. Wiebe LI, Knaus EE, Morin KW. Radiolabelled pyrimidine nucleosides to monitor the expression of HSV-1 thymidine kinase in gene therapy. *Nucleosides Nucleotides* 1999; 18:1065–1066.
17. Morin KW, Atrazheva ED, Knaus EE, Wiebe LI. Synthesis and cellular uptake of 2'-substituted analogues of (E)-5-(2-[ $^{125}\text{I}$ ]iodovinyl)-2'-deoxyuridine in tumor cells transduced with the herpes simplex type-1 thymidine kinase gene. Evaluation as probes for monitoring gene therapy. *J Med Chem* 1997; 40:2184–2190.
18. Bakker WH, Breeman WA, van der Pluijm ME, de Jong M, Visser TJ, Krenning EP. Iodine-131 labelled octreotide: not an option for somatostatin receptor therapy. *Eur J Nucl Med* 1996; 23:775–781.
19. Vincent AJ, Vogels R, Someren GV, et al. Herpes simplex virus thymidine kinase gene therapy for rat malignant brain tumors. *Hum Gene Ther* 1996; 7:197–205.
20. Boshart M, Weber F, Jahn G, Dorsch-Hasler K, Fleckenstein B, Schaffner W. A very strong enhancer is located upstream of an immediate early gene of human cytomegalovirus. *Cell* 1985; 41:521–530.
21. Nanda D, Vogels R, Havenga M, Avezaat C, Bout A, Sillevs Smitt P. Treatment of malignant gliomas with a replication competent adenoviral vectors. In: The Fourth Annual Meeting of the American Society of Gene Therapy, 2001. Seattle: Molecular Therapy; 2001:abstract 988.
22. Fallaux FJ, Bout A, van der Velde I, et al. New helper cells and matched early region 1-deleted adenovirus vectors prevent



- generation of replication-competent adenoviruses. *Hum Gene Ther* 1998; 9:1909–1917.
23. Shabram PW, Giroux DD, Goudreau AM, et al. Analytical anion-exchange HPLC of recombinant type-5 adenoviral particles. *Hum Gene Ther* 1997; 8:453–465.
  24. Fallaux FJ, Kranenburg O, Cramer SJ, et al. Characterization of 911: a new helper cell line for the titration and propagation of early region 1-deleted adenoviral vectors. *Hum Gene Ther* 1996; 7:215–222.
  25. Mercer JR, Xu LH, Knaus EE, Wiebe LI. Synthesis and tumor uptake of 5-<sup>82</sup>Br- and 5-<sup>131</sup>I-labeled 5-halo-1-(2-fluoro-2-deoxy-beta-D-ribofuranosyl)uracils. *J Med Chem* 1989; 32:1289–1294.
  26. Bradford MM. A rapid and sensitive method for the quantitation of microgram quantities of protein utilizing the principle of protein-dye binding. *Anal Biochem* 1976; 72:248–254.
  27. Kamel-Reid S, Dick JE. Engraftment of immune-deficient mice with human hematopoietic stem cells. *Science* 1988; 242:1706–1709.
  28. Wildner O, Blaese RM, Morris JC. Synergy between the herpes simplex virus tk/ganciclovir prodrug suicide system and the topoisomerase I inhibitor topotecan. *Hum Gene Ther* 1999; 10:2679–2687.
  29. Contag CH, Spilman SD, Contag PR, et al. Visualizing gene expression in living mammals using a bioluminescent reporter. *Photochem Photobiol* 1997; 66:523–531.
  30. Bell JD, Taylor-Robinson SD. Assessing gene expression in vivo: magnetic resonance imaging and spectroscopy. *Gene Ther* 2000; 7:1259–1264.
  31. Zinn KR, Buchsbaum DJ, Chaudhuri TR, Mountz JM, Grizzle WE, Rogers BE. Noninvasive monitoring of gene transfer using a reporter receptor imaged with a high-affinity peptide radiolabeled with <sup>99m</sup>Tc or <sup>188</sup>Re. *J Nucl Med* 2000; 41:887–895.
  32. MacLaren DC, Gambhir SS, Satyamurthy N, et al. Repetitive, non-invasive imaging of the dopamine D2 receptor as a reporter gene in living animals. *Gene Ther* 1999; 6:785–791.
  33. Brust P, Haubner R, Friedrich A, et al. Comparison of [<sup>18</sup>F]FHPG and [<sup>124</sup>/<sup>125</sup>I]FIAU for imaging herpes simplex virus type 1 thymidine kinase gene expression. *Eur J Nucl Med* 2001; 28:721–729.
  34. Jacobs A, Tjuvajev JG, Dubrovin M, et al. Positron emission tomography-based imaging of transgene expression mediated by replication-conditional, oncolytic herpes simplex virus type 1 mutant vectors in vivo. *Cancer Res* 2001; 61:2983–2995.
  35. Jacobs A, Braunlich I, Graf R, et al. Quantitative kinetics of <sup>124</sup>I-FIAU in cat and man. *J Nucl Med* 2001; 42:467–475.
  36. Nanda D, Vogels R, Havenga M, Avezaat C, Bout A, Sillevius Smitt P. Treatment of malignant gliomas with a replicating adenoviral vector expressing herpes simplex virus-thymidine kinase. *Cancer Res* 2001; 61:8743–8750.